Integrated cascade biorefinery processes for the production of single cell oil by *Lipomyces starkeyi* from *Arundo donax*L. hydrolysates

Nicola Di Fidio[a*], Giorgio Ragaglini[b*], Federico Dragoni[b,c], Claudia Antonetti[a], Anna Maria Raspolli Galletti[a]

[a]*Department of Chemistry and Industrial Chemistry, University of Pisa, Via G. Moruzzi 13, 56124 Pisa, Italy.*

[b]*Institute of Life Sciences, Sant'Anna School of Advanced Study, Piazza Martiri della Libertà 33, 56127 Pisa, Italy.*

[c]*Leibniz Institute for Agricultural Engineering and Bioeconomy (ATB), Department of Technology Assessment and Substance Cycles, Potsdam-Bornime.V. Max-Eyth-Allee 100, 14469 Potsdam, Germany.*

[*]Corresponding author: Giorgio Ragaglini

E-mail address: g.ragaglini@santannapisa.it

Telephone: +39 050 883512

*Co-corresponding author: Nicola Di Fidio

E-mail address: n.difidio@studenti.unipi.it

Telephone: +39 050 2219290

ABSTRACT

Giant reed (*Arundo donax* L.) is a promising source of carbohydrates that can be converted into single cell oil (SCO) by oleaginous yeasts. Microbial conversion of both hemicellulose and cellulose fractions represents the key step for increasing the economic sustainability for SCO production. *Lipomyces starkeyi* DSM 70296 was cultivated in two xylose-rich hydrolysates, obtained by the microwave-assisted hydrolysis of hemicellulose catalysed by $FeCl_3$ or Amberlyst-70, and in two glucose-rich hydrolysates obtained by the enzymatic hydrolysis of cellulose.*L. starkeyi* grew on both undetoxified and partially-detoxified hydrolysates, achieving the lipid content of 30 wt% and yield values in the range 15-24 wt%. For both integrated cascade processes the final production of about 8 g SCO from 100 g biomass was achieved. SCO production through integrated hydrolysis cascade processes represents a promising solution for the effective exploitation of lignocellulosic feedstock from perennial grasses towards new generation biodiesel and other valuable bio-based products.

Keywords: Glucose- and xylose-rich hydrolysates; Yeast fermentation; Biodiesel; Lignocellulosic feedstock; Perennial grasses.

1. Introduction

The transition from a fossil-based economy to a bio-based one is a current global goal in order to contrast some important issues such as climate change and environmental pollution and to reduce the dependency on fossil sources as well. Thus, the replacement of fossil fuels and materials with biofuels and bioproducts represents the key solution.Among biofuels, biodiesel is one of the most promising renewable

energy sources since it does not require new technology and engines for its use(d'Espaux et al., 2015). Conventional biodiesel is produced on an industrial scale starting from vegetable oils obtained from oleaginous crops. However, most of the high productivity oleaginous plant species are food crops, thus determining the ethical debate on the right use of these renewable resources due to the competition between the energy industry and food chain(Mahlia et al., 2020). An innovative and promising solution is represented by new generation biodiesel, produced from microbial oil or single cell oil (SCO)(Patel et al., 2020). Some oleaginous yeasts can accumulate lipids over 20% of their dry cell weight and the typical lipids profile of SCOs is very similar to that of the main vegetable oils such as palm oil, rapeseed oil and sunflower oil(Patel et al., 2020). Moreover, SCO from oleaginous yeastsrepresents a source of platform chemicals for several biobased products, such as surfactants, lubricants, food additives, plastics, paints and detergents(Probst et al., 2016). Among oleaginous yeasts, *Lipomyces starkeyi* can afford high lipid yields from both hexoses and pentoses, re-utilising small amounts of its intracellular lipids, showing the capability to grow in simple media (e.g. without vitamin supplementation) and to carry out extracellular polysaccharide degradation, as well as good tolerance to inhibitory compounds such asaldehydes, alcohols and organic acids (Sutanto et al., 2018; Wang et al., 2014). For these reasons,*L. starkeyi* is a well-known, promising oleaginous yeastfor industrial-scale production of SCO. Nevertheless, thecurrent high prices of most conventional carbon sources (e.g.sugars)stronglylimit the economic competitiveness of SCO respect to crude oil(Javaid et al., 2017). Conversely, lignocellulosic feedstocks obtained from crop residues or high-yielding and resource-efficient perennial grasses, such as giant reed

71 (*Arundo donax* L.),can be less expensive and reduce the competition with food crops,
72 potentially leading to more sustainable pathways for SCO production.
73 As a biomass crop, giant reed is characterised by several positive traits: it is a
74 perennial species, thus avoiding annual soil tillage; it has shown high yielding potential
75 under low input management systems, even on marginal, contaminated or underutilised
76 lands without irrigation; it effectively removes nitrates from the soil, helping to mitigate
77 nitrate pollution risk (e.g. in riparian buffer strips); it does not suffer from any major
78 pathogen or pest(Bosco et al., 2016; Ceotto et al., 2018; Scordia & Cosentino, 2019).
79 Moreover, giant reed biomass can be collected from spontaneous riparian stands, in
80 order to maintain riverbanks and mitigate the flooding risk, or to control populations
81 where this species is considered invasive (e.g. North America) (Pilu et al., 2014).Giant
82 reed is typically rich in both cellulose (about 40% of dry matter) and hemicellulose
83 (about 25% of dry matter)(Nassi o Di Nasso et al., 2011)and presents high reactivity in
84 the hydrothermal conversion thus offering outstanding perspectives for the conversion
85 into chemicals and biofuels.The hemicellulose fraction (the second most abundant
86 polysaccharide in lignocellulosic biomass) is usually wasted in traditional
87 biorefineryplants, where it is generally removed during the pretreatment of the biomass
88 in order to reduce structural constraints on the enzymatic hydrolysis of cellulose (Xavier
89 et al., 2017). In particular, during conventional pretreatments based on organic and
90 inorganic acids, alkali, hot water, steam and ammonia explosion, and ionic liquids,
91 hemicellulose is decomposed in by-products that represent strong inhibitors in the
92 hydrolysate conversion through the fermentation route. Thus, the complete recovery by
93 selective fractionation of the hemicellulose componentinto sugars to be fermented
94 would significantly improve the economic balance of biofuels and bioproducts

production. Alternative pathways ofselective microwave-assisted hydrolysis have been already demonstrated effective in providing xylose-rich hydrolysates from the hemicellulose fraction of giant reed biomass (Di Fidio et al., 2019; Di Fidio et al., 2020c), while the cellulose-rich residues can be source of glucose-rich hydrolysates by means of enzymatic hydrolysis (Di Fidio et al., 2020b; Di Fidio et al., 2020c).

The present study evaluatesa novel integrated cascade biorefinery scheme for the production of SCO by *L. starkeyi*DSM 70296 in batch-mode fermentation of both xylose- and glucose-rich hydrolysates. In order to verify the effectiveness of this approach on different types of xylose- and glucose-rich hydrolysates, these last wereobtained adopting two different cascade processes both for hemicellulose and for cellulose fractions hydrolysis.As widely reported in the literature, the pretreatment step is expensive, energy-intensive and, often adopts chemicals which require special disposal, handling, or production methods. All these aspects often compromise the economic sustainability of a biorefinery process on an industrial scale (Yang et al., 2018). Therefore, in the present study,the different hydrolysateswere obtained from unpretreated giant reed biomass in order to assesstheir conversion to give SCO,by evaluating: 1) the efficiency of conversion by *L. starkeyi*DSM 70296 of both xylose- and glucose-rich hydrolysates obtained by catalytic and enzymatic conversion respectively; 2) the mass balance of the investigatedcascade processes; 3) the fatty acids composition of the obtained SCO.

2. Materials and methods

2.1.Feedstock and materials

Giant reed (*Arundo donax* L.) biomass was collected from a mature, 4-year old plantation, routinely managed by yearly harvests, at the Centre for Agri-environmental Research "Enrico Avanzi" of the University of Pisa in San Piero a Grado (Pisa, latitude 43° 68' N, longitude 10° 35' E). In December 2018, giant reed biomass was harvested and then treated and characterisedas described in our previous work (Di Fidio et al., 2019). After the harvesting, whole culms and leaves were ground in 1.0 mm average size particles, dried at 105 °C in an oven until a constant weight, and then stored in a desiccator up to their use.

The feedstock contained 36.3±0.4 wt% glucan, 17.3±0.2 wt% xylan, 1.9±0.1wt% arabinan, 0.6±0.0 wt% mannan, 3.6±0.1 wt% acetyl groups, 2.0±0.1 wt% ash, 15.4±0.8 wt%extractives, 22.0±0.3 wt%acid-insoluble lignin, 0.9±0.1wt% acid-soluble lignin.Values represent the mean, n = 3, ±standard deviation.

Chemicals of analytical purity grade were provided by Sigma-Aldrich (USA). Novozymes (Denmark)kindly provided the enzymatic mixture Cellic® CTec2.

2.2 Hemicellulose and cellulose hydrolysis

SCO production by *L. starkeyi*DSM 70296 was evaluated in batch-mode fermentation of xylose- and glucose-rich hydrolysates obtained from two different cascade processes based on two consecutive steps for hemicellulose and cellulose hydrolysis, respectively.

Under the first process, a xylose-rich hydrolysate (X1) was obtained by the selective microwave-assisted hydrolysis of hemicellulose performed in the monomodal microwave reactor CEM Discover S-class System by employing the homogeneous catalyst$FeCl_3$,adoptingthe following reaction conditions: 9 wt% biomass loading, 150

°C, 2.5 min and $FeCl_3$/giant reed weight ratio 0.17 wt/wt (Di Fidio et al., 2019). In particular, 1 g of raw biomass was charged in the glass vessel (35 mL) containing 10 mL H_2O and about 0.28 g $FeCl_3$. The microwave reactor was heated at 150 °C and the reaction was carried out for the required time under magnetic stirring. At the end of the reaction, the vessel was rapidly cooled at room temperature through an external airflow.

According to the second approach, xylose-rich hydrolysate (X2) was produced by the selective microwave-assisted hydrolysis of hemicellulose performed in the monomodal microwave reactor CEM Discover S-class System by employingthe heterogeneous catalystAmberlyst-70, adopting the following reaction conditions: 17 wt% biomass loading, 160 °C, 20 min, Amberlyst-70/giant reed weight ratio 0.20 wt/wt(Di Fidio et al., 2020c).In particular, 4.1 g of raw biomass was charged in the glass vessel (35 mL) containing 20 mL H_2O and about 0.4 g Amberlyst-70. The microwave reactor was heated at 150 °C and the reaction was carried out for the required time under magnetic stirring. At the end of the reaction, the vessel was rapidly cooled at room temperature through an external airflow.At the end of the reaction, the liquid fraction, containing a high concentration of xylose and a low concentration of glucose, was recovered by filtration under vacuum on a Gooch filter and analysed by HPLC. In order to adapt X2 to the yeast growth condition,theselective removal of furfural (1.0 g/L) and acetic acid (4.7 g/L) was performed by vacuum evaporation (Sutanto et al., 2018). The solution was firstly concentrated in a laboratoryrotavapor vacuum system at 8 kPa, 80 rpm and 50 °C for 1 h and then diluted up to the starting concentration values of sugars by adding deionised water. The final composition of X2 used as fermentation medium was the following one (g/L): glucose 8.0, xylose 38.0, 5-HMF 1.3, formic acid 1.0, levulinic acid 0.5.

The separated solid residues obtained by the first step, namely the cellulose-rich residues (CRR1 and CRR2), werewashed with deionized water, oven-dried at 105 °C and then used as the substrate for the following enzymatic hydrolysis of the cellulose fraction. The enzymatic activity of the commercial preparation Cellic® CTec2 (a mixtureof endo- and exocellulase, β-glucosidases and hemicellulase) was equal to 134.5 FPU/mL. The enzymatic hydrolysis was carried out in a 150 mL flask adopting the following reaction conditions: pH 4.8, 50 °C, 50 mL of the 0.05 M citrate buffer solution, 25 FPU/g glucan Cellic® CTec2, shaking at 160 rpm.At the end of the reaction, the glucose-rich hydrolysate was recovered by filtration under vacuum on a Gooch filter and analysed by HPLC (Di Fidio et al., 2020b; Di Fidio et al., 2020c).Therefore, two different glucose-rich hydrolysates (Table 1) were obtained: the first one by the enzymatic hydrolysis of the CRR recovered after the $FeCl_3$-catalysed hydrolysis of hemicellulose (G1) and the second one after the Amberlyst-70-catalysed hydrolysis of hemicellulose (G2),adoptingin both cases the following reaction conditions: 9 wt% biomass loading, 50 °C, 96 h and 25 FPU/g glucan Cellic® CTec2.

The quantification of glucose, xylose, acetic acid, formic acid, levulinic acid, 5-hydroxymethylfurfural and furfural was performed by High Performance Liquid Chromatography (HPLC) PerkinElmer Flexar Isocratic Platform equipped with a differential refractive index detector(Di Fidio et al., 2019).

2.3. Yeast strain and cultivation

The oleaginous yeast strain *Lipomyces starkeyi* DSM 70296 was provided by DSMZ (Germany). Preparation, sterilisation and inoculation of preculture media were performed as previously reported(Di Fidio et al., 2020a). A calculated volume ofthe

190 preculture was added to the fermentation medium in order to reach the inoculum
191 concentration of 5.0 g/L dry cell weight (DCW).
192
193 *2.4.Bioconversion of sugars into single cell oil*
194 Batch-mode fermentations were carried out according to the process conditions
195 previously described (Di Fidio et al., 2020a). Briefly, 50 mL of undetoxified
196 lignocellulosic hydrolysate was set as the working volume in 250 mL Erlenmeyer flasks
197 at 30 °C, pH 5.5 and speed of 180 rpm. The C/N weight ratio was 40 and yeast extract
198 was selected as nitrogen and vitamins source, according to the literature on *L.*
199 *starkeyi*(Sutanto et al., 2018; Zhao et al., 2008).The selected C/N weight ratio was
200 obtained by adding a proper amount of yeast extract as a function of the carbon content
201 of each hydrolysate. Both xylose- and glucose-rich hydrolysates were supplemented
202 with nutrients and all fermentation media were sterilised by microfiltration (0.22 μm).
203 *L. starkeyi* cultivation wasstopped when the complete depletion of sugars in the media
204 was reached, in order to avoid the use of accumulated lipids as a carbon source by the
205 yeast. Each test was replicated three times.
206 In order to monitor the yeast growth, sugars concentration and intracellular lipid
207 content during batch fermentations, every 24 h two samples of 1 mL were withdrawn
208 and centrifuged in order to perform DCWdetermination, HPLC analysis and lipids
209 extraction and quantification.
210
211 *2.5. Single cell oil extraction and FAMEs determination*
212 During and at the end of fermentations, yeast cells were harvested by centrifugation
213 (8,000 ×gfor 10 min), washed twicewith distilled water, lyophilised, and stored in a

desiccator until the SCO extraction was carried out(Di Fidio et al., 2020a).The lipid yield was calculated by means of the following equation:

$$Y_L = (C_L/C_s)\cdot 100$$

where Y_L is the lipid yield (wt%), C_L is the final lipids concentration (g/L) and C_s is the concentration (g/L) of total consumed sugars at the end of the fermentation.

The lipid content (wt%, C_L)was calculated by means of the following equation:

$$C_L = (m_L/m_{cells})\cdot 100$$

where m_L is the amount of the lipids (g) and m_{cells} is the amount of lyophilised yeast biomass (g).

The chemical characterisation of SCO was performed by GC-FID analysis after the direct transmethylation of microbial triglycerides into fatty acids methyl esters (FAMEs)(Di Fidio et al., 2020a).

2.6. Statistical analysis

Statistical analysis of the results obtained from the batch-mode fermentation of X1, X2, G1 and G2 hydrolysates was performed by a two-way analysis of variance (ANOVA) according to a completely randomised design. The type of hydrolysate and the process time were set as factors, while sugars concentrations, DCW concentration, lipid content,lipids production and lipids production rate were considered as dependent variables. Moreover, a one-way ANOVA was performed selecting the type of hydrolysate as factor and DCW concentration, lipid content, lipids production and the maximum lipids production rate were set as dependent variables.

3. Results and discussion

3.1.Fermentation of xylose-rich hydrolysates

In the present study, two xylose-rich hydrolysates (X1 and X2),obtained from the hydrolysis of the unpretreated giant reed adopting two different catalytic systems, one homogeneous and the other heterogeneous, were tested as the carbon source for the production of new generation oil. Figure 1shows the general flow chart of the adopted cascade processes, while the composition of the starting hydrolysates is reported in Table 1.

(Figure 1, near here)

(Table 1, near here)

X1 was produced from the hydrolysis reaction catalysed by the homogeneous catalyst $FeCl_3$, which presents important advantages comparedwith traditional strong homogeneous inorganic acids, such as less corrosion of reactor, low cost, simple recovery by precipitation, good efficacy at mild reaction conditions, energy-saving, and high selectivity (Loow et al., 2015). On the other hand,X2 was obtained from the hydrolysis reaction catalysed by the heterogeneous catalyst Amberlyst-70, a promising styrene-based sulfonic acid resin for biomass hydrolysis (Qi et al., 2019), in order to evaluate the potentiality of the products obtained by hydrolysis with different catalytic approaches. In fact, the adoption of this heterogeneous system allowseasy and safe operations with minor corrosion problems, simple recovery of the catalyst with less waste disposal, catalyst recycle with the maintenance of the catalytic performance(Meena et al., 2015).Nonetheless, a previous optimisation study evidenced that the heterogeneous catalyst requires higher reaction temperature and longer times than $FeCl_3$, thus causing the presence in the X2 hydrolysate of potential inhibitors,as furanic derivatives and acetic acid (Di Fidio et al., 2020c).

The results of the batch fermentation of the undetoxified lignocellulosic hydrolysate X1 by *L. starkeyi*are reported in Figure 2A.

(Figure 2, near here)

In this case, in the first 24 h, the growth phase was not observed, while from 24 to 72 h the yeast growth significantly increased.The net production of DCW was 11 g/L. It ranged from the starting value of 5 g/L to the final concentration of 16 g/L. The sugars content decreased from 24 to 72 h as the increasing DCW. In particular,the consumption of glucose and xylose was simultaneous, due to the relatively low initial concentration of glucose (5.6 g/L) in the fermentation medium. These results confirmed the ability of *L. starkeyi* to convert xylose into SCO.This important feature is crucial for the complete biological conversion of the second-generation sugars obtainable fromgiant reed into microbial oil, increasing the profitability of the proposed biorefinery scheme.At 72 h, the complete consumption of both glucose and xylose was observed, thus indicating the end of fermentation. The intracellular lipid content ranged from 10 to about 30 wt% during the fermentation. It was 10% at 0 h and around 30% at 72 h.Moreover, the maximum oil productivity, 2.8 g/L/d, was observed in the last stage between 48 and 72 h.In the X1 fermentation, 25 g/L of total reducing sugars were converted into 4.6 g/L of lipids, achieving the lipid yield of 18.6wt%.

According to the stoichiometry of biochemical conversion of glucose and xylose into triacylglycerols in most oleaginous yeasts, the maximum theoretical yield is around 33 wt%(Papanikolaou & Aggelis, 2011). However, in the lipogenesis pathway of *L. starkeyi* cytosolic malic enzyme takes NAD^+ as coenzyme rather than $NADP^+$, determining the lower availability of NADPH in the cytosol, which is one of the key factors for the synthesis of the lipids. As a consequence, in *L. starkeyi*the maximum

theoretical yieldis 27.6 wt%(Sutanto et al., 2018). On this basis, the obtained yield of 18.6 wt% represented 67.4% of the maximum theoretical yield for this species. Moreover, in the literature, the experimentallipid yields obtained both in synthetic and biomass-derived media rangedfrom 10 and 24 wt%,thus attesting the achieved value as around 80% of the maximum experimental yield obtained up to now from*L. starkeyi*(Sutanto et al., 2018).

On the other hand, after a preliminary test, *L. starkeyi*showed to be not suited for growing on the xylose-rich hydrolysate X2 as obtained from the selective microwave-assisted Amberlyst-70-catalysed hydrolysis,due to the presence of a relatively high concentration of furfural, HMF and acetic acid (Table 1). The presence of undesired by-products was due to the adoption of the high-gravity approach in the hemicellulose hydrolysis catalysed by Amberlyst-70 which allowed us to use the biomass loading of 200 g/L (17 wt%). This high-gravity approach increases the economic sustainability of the sugars production, despite a slight increase in by-products synthesis.For this reason, furfural and acetic acid were removed by vacuum evaporation and the obtained concentrated hydrolysate, containing 16.0 g/L glucose, 76.0g/L xylose, 2.6 g/L 5-HMF, 1.0 g/L levulinic acid, was tested. Also in this case the yeast was not able to grow, almost surely due to the increased concentration of 5-HMF and other unidentified by-products. After the dilution of the hydrolysate in order to restore the initial concentration of both reducing sugars and other by-products (8.0 g/L glucose, 38.0g/L xylose, 1.3 g/L 5-HMF, 0.5 g/L levulinic acid), the fermentation was successfully carried out. Figure 2B shows the results of the batch-mode fermentation of the processed X2 furfural-free hydrolysate by *L. starkeyi*.

Similarly to the fermentation of X1, the yeast growth did not occur in the first 24 h. From 24 to 48 h a slight yeast growth was observed, while the major growth phase evolved from 48 to 72 h.The bioconversion of X2 required a longer time than X1 (96 vs 72 h), due to the higher concentration of total reducing sugars (46 vs 25 g/L). The net production of DCW was 19.1 g/L, which resulted higher respect to the value (11 g/L) of the previous case. It ranged from the starting value of 4.9 g/L to the final concentration of 24 g/L. The sugars consumption evolved according to the DCW increase, being slower between 24 and 48 h and 72 and 96 h and faster during the growth phase observed from 48 to 72 h.Compared to X1, the consumption of glucose and xylose was asynchronous. Indeed, glucose depletionstarted earlier, already during the lag phase of DCW growth, and its complete consumption required almost half the time of xylose.Despite the lower initial content, the consumption of glucose evolved faster, beingthe favoured carbon source for oleaginous yeasts(Zhao et al., 2008). Instead, the consumption of xylose started after 24 h. Therefore, the mainphase of xylose decrease was also observed 24 h later and its complete consumption was delayed at 96 h. The final lipid content was 28 wt%, while the maximum oil productivity, calculated in the major growth phase (48–72 h), resulted 4.1 g/L/d.This value was higher than the maximum productivity reached in the previous case because of the higher cell biomass production (DCW). In X2 fermentation, 46 g/L of total reducing sugars were converted into 6.7 g/L of lipids, achieving the lipid yield of 14.6 wt%. The obtained yield represented 52.9% of the maximum theoretical yield and 60.8% of the maximum experimental yield for *L. starkeyi*(Sutanto et al., 2018). These values resulted lower than those reached in X1 despite the consumption of a double amount of reducing sugars. This result can be related to the presence of a higher concentration of by-products, such

as 5-HMF and organic acids, in X2 than in X1, generating stressful growing conditions for the yeast which hampered the lipogenesis. Moreover, the presence of Fe^{3+} in X1,due to the use of $FeCl_3$ as a homogeneous acid catalyst for the hydrolysis of the giant reed hemicellulose into xylose, is reported to favour the lipid production in oleaginous yeasts (Gong et al., 2014; Zhao et al., 2008).

The cell biomass productions(DCW) ascertained in the X1 and X2 fermentations agreed with the concentrations of 12.3 g/L reported by Tapia et al. (Tapia et al., 2012) and 13.6 g/L reported by Leiva et al. (Leiva-Candia et al., 2015) for the same yeast strain DSM 70296 cultivated in a flask on pure xylose and glucose, respectively. Moreover, the DCW concentration achieved in the present investigation on the xylose-richgiant reed hydrolysate was higher respect to the maximum value of 10 g/L reported by Pirozzi et al. (Pirozzi et al., 2015) on diluted giant reed hydrolysate obtained by H_2SO_4-catalysed hydrolysis.

In both X1 and X2 fermentations, the starting lipid content (10 wt%) agreed with those reported in the literature for the *L. starkeyi*(Wang et al., 2014), while the final values (around 30 wt%) resulted higher respect to the literature data reported in all the other fermentation experimentson giant reed hydrolysates, obtained by different pretreatments and catalytic approaches, by using the same yeast strain (Pirozzi et al., 2014a; Pirozzi et al., 2015; Pirozzi et al., 2014b).

Considering the fermentation of other kinds of lignocellulosic hydrolysates by the same yeast, Xavier et al. reported the lipid yield of 14.0 wt% employing sugarcane bagasse hydrolysate (Xavier et al., 2017). Azad et al. claimed the lipid yield of 18.0 wt% using rice straw hydrolysate (Azad et al., 2014), whilst Calvey et al. obtained the lipid yield of 14.0 wt% adopting corn stover hydrolysate (Calvey et al., 2016). Moreover, considering

357 the batch-mode fermentation of pure xylose or a combination of xylose and glucose,
358 Tapia et al. reported the lipid yield of 14 wt% in the presence of 30 g/L xylose adopting
359 the C/N weight ratio of 50 (Tapia et al., 2012), while Anschau et al. obtained the lipid
360 yield of 10 wt% in the presence of 42 g/L xylose and 18 g/L glucose with the C/N
361 weight ratio of 50 (Anschau et al., 2014).
362 All the obtained results confirmed the feasibility of the SCO production from the
363 hemicellulose fraction of giant reed after its selective hydrolysis by means of both
364 homogeneous and heterogeneous acid catalysts. Moreover, the ascertained SCO yields
365 make this approach surely competitive respect tothe up to now reported literatureones
366 where synthetic model solutionsor hydrolysates obtained from pretreated lignocellulosic
367 biomasses are adopted as substratesfor fermentation.
368
369 *3.2.Fermentation of glucose-rich hydrolysates*
370 In the perspective of the complete valorisation of the carbohydrates present in the
371 starting biomass, theglucose-rich hydrolysates G1 and G2 (Table 1), obtained from the
372 hydrolysis of the giant reed cellulose-rich residuesCCR1 and CCR2 remaining after the
373 two different catalytic hemicellulose dissolutions were employedas a carbon source for
374 the production of SCO (Figure 1). For the production of G1 and G2 from the cellulose-
375 rich solids, theenzymatic hydrolysiswas preferred because ensured the selective
376 depolymerisation of the cellulose into glucoseavoiding the formation of toxic inhibitors
377 for the *L. starkeyi* growth. Figure 2C shows the results of the batch-mode fermentation
378 of G1 by *L. starkeyi*.
379 The absence of inhibitors in the hydrolysate allowed the prompt yeast growth in the first
380 24 h. From 24 to 48 h the majorgrowth was observed, while from 48 to 72 h *L. starkeyi*

reached the stationary phase.With respect to the previous fermentations, the absence of a long lag phase (at least 24 h) decreased the productive processing time from 72 and 96 h ofX1 and X2, respectively, to 48 h observed in G1. In the latter, the DCW concentrationmoved from the starting value of 4.8 g/L to the final concentration of 17.1 g/L.The net production of DCW was 12.3 g/L, similar to the value (11 g/L) obtained in the X1 fermentation, due to the comparable total reducing sugars concentration.The glucose consumption was consistent with the cell biomass growth. It started during the first 24 h and ended after 72 h, even if just after 48 h the glucose concentration in the G1 was only 1.6 g/L. The lipid content varied from about 10 to 31 wt%. Moreover, the maximum oil productivity, calculated in the major growth phase (24–48 h), resulted 3.5 g/L/d which represented an intermediate result with respect to the values obtained by fermenting X1 and X2.In the G1fermentation, 21.8 g/L of total reducing sugars were converted into 5.3 g/L of lipids, achieving the lipid yield of 24.3 wt%. The obtained yield represented 88.0% of the maximum theoretical yield and 100% of the maximum experimental yield for *L. starkeyi* on synthetic and biomass-derived media (Sutanto et al., 2018). These values resulted higher than those reached in X1 and X2 fermentationsdue to the presence of glucose as sole carbon source and the absence of the hydrolysis reaction by-productsdue to the adoption of the enzymatic catalytic approach. In fact, these process conditions favoured the lipogenesis, increasing the lipid yield in the *L. starkeyi* DSM 70296.

Figure 2D shows the results of the batch-mode fermentation of G2 by *L. starkeyi*.Similarly to G1fermentation, the yeast growth started already during the first 24 h without a significant lag phase due to the high quality of the hydrolysate related to the improvedcatalytic strategy based on the highly selective enzymatic hydrolysis. The

405 major growth phase took place from 24 to 48 h while during the last 24 h of the process
406 a slight yeast growth evolved towards the stationary phase.DCW concentration ranged
407 from the starting value of 5.1 to 22.0 g/L at process end. The net increase of DCW was
408 16.9 g/L, which resulted the maximum value obtained in the present investigation. The
409 glucose consumption was consistent with the DCW growth. It started within 24 h and
410 ended after 72 h. The lipid content ranged from about 10 to 34 wt%. Moreover, the
411 maximum oil productivity, observed during themajorgrowth phase (24–48 h), 4.4
412 g/L/d,was higherthan the value obtained fromG1and similar to that achievedfromX2. In
413 G2fermentation, 32.8 g/L of total reducing sugars were converted into 7.5 g/L of lipids,
414 achieving the lipid yield of 22.9 wt%. The obtained yield represented the 83.0% of the
415 maximum theoretical yield and the 95.4% of the maximum experimental yield for *L.*
416 *starkeyi* on synthetic and biomass-derived media (Sutanto et al., 2018), in agreement
417 withthe results achieved in the previous fermentation of the glucose-rich hydrolysate
418 G1.
419 In G1 fermentation, the final cell biomass productionwas similar to the value of 12.3
420 g/L achieved on the sole pure glucose in flask by Leiva-Candia et al. (Leiva-Candia et
421 al., 2015) for the same yeast strain with the C/N equal to 50. On the contrary, it resulted
422 higher than the value of 9.4 g/L obtained on the sole pure glucose by Angerbauer et al.
423 (Angerbauer et al., 2008) working with a C/N equal to 150, which favoured the
424 lipogenesis and limited the yeast growth. In G2 fermentation, the final cell biomass
425 production was similar to the value of 21.2 g/L obtained by Bonturi et al. on pure
426 glucose (Bonturi et al., 2015). Moreover, in both G1 and G2 fermentation, the biomass
427 production was significantly higher than the maximum value of 10 g/L reached on the
428 glucose-rich giant reed hydrolysate obtained by H_2SO_4-catalysed hydrolysis(Pirozzi et

al., 2015). Considering the fermentation of other lignocellulosic hydrolysates, the DCW production was similar to those obtained on sugarcane bagasse (Anschau et al., 2014; Xavier & Franco, 2014), Brazilian molasses (Vieira et al., 2014) and sunflower meal (Leiva-Candia et al., 2015).

As previously observed for X1 and X2 fermentation, also in both G1 and G2 fermentations, the lipid content resulted higher respect to the range of 17-21 wt% achieved by fermenting giant reed hydrolysates obtained by different catalytic strategies (Pirozzi et al., 2014a; Pirozzi et al., 2015; Pirozzi et al., 2014b).

Figure 3 shows the results of the statistical analysis (one-way ANOVA) of the findings obtained from the fermentation of X1, X2, G1 and G2. In particular, DCW and lipids concentration, lipid content and the maximum lipids production rate were compared as a function of the type of the hydrolysate.

(Figure 3, near here)

Regarding the DCW production, X1 and G1 were not significantly different from each other, as well as X2 and G2, but these last two values were significantly higher than those obtained for X1 and G1. Regarding the lipids concentration, the values obtained for X1 resulted significantly lower than those obtained for X2 and G2. The lipids concentration obtained from the fermentation of G1 was not significantly different with respect to the values reached for X1 and X2, while it was significantly lower than G2. Considering the lipid content, not statistically differences were observed between X1 and X2, as well as between G1 and G2. The only statistically difference was observed between G2 and X1/X2.Considering the maximum lipids production rate, the values achieved for X2 and G2 were not statistically different from each other, but they were

significantly higher than those obtained for X1. The value reached in the case of G1 was not significantly different respect to all the other results.

Both the homogeneous and the heterogeneous catalytic approaches for the first process step allowed the production of cellulose-rich residuessuitable for the subsequent enzymatic hydrolysis, which provided good-quality glucose-rich hydrolysates. The good performances of *L. starkeyi*in theirsuccessive fermentation confirmed the profitability of the SCO production from the cellulose fraction of giant reed following the cascade biorefinery scheme presented in this work.

3.3.Fatty acids composition of single cell oils

The fatty acids composition of microbial oils is strongly affected by the main process parameters, such as the nature of the carbon and nitrogen source, the carbon to nitrogen weight ratio, the sugars concentration, the fermentation mode, the nature and the concentration of growth inhibitors and the yeast species and strain (Pirozzi et al., 2015; Sutanto et al., 2018; Takaku et al., 2020; Wild et al., 2010). In the present investigation, the lipid profiles of the SCO produced by *L. starkeyi* DSM 70296 were listed in Table 2.

(Table 2, near here)

They were characterised by a good percentage (~55 wt%) of unsaturated long-chain fatty acids according to the literature (Gong et al., 2012; Pirozzi et al., 2015; Xavier & Franco, 2014).In particular, the SCO profiles achieved by the fermentation of X1 and X2 agreed with those obtained by other studies on the xylose-rich hydrolysates or synthetic media (Gong et al., 2012; Wang et al., 2014; Xavier et al., 2017). The oils obtained by the bioconversion of G1 andG2 resulted in agreement with those derived from the fermentation of glucose-rich hydrolysates or synthetic media (Gong et al.,

476 2012; Pirozzi et al., 2014a; Wang et al., 2014). Comparing the lipid profiles obtained in
477 each process configuration of this study, the chemical composition of the SCO produced
478 by *L. starkeyi* on the various xylose- or glucose-rich hydrolysates is quite constant. This
479 result can be explained by considering the use of the same yeast strain, C/N ratio,
480 nitrogen source (yeast extract) and fermentation-mode, together with the low
481 concentration of growth inhibitors such as 5-HMF and furfural, the limited range of
482 sugars concentrations (22-46 g/L) and the similar carbon source (glucose and xylose).
483 Moreover, in vegetable and microbial oils, the presence of unsaturated fattyacids favour
484 the cold properties,such as the cloud point, thepour point and the cold filter plugging
485 point. At the same time, these components reduce the oxidation stability(Pirozzi et al.,
486 2015; Serrano et al., 2014). However, the presence of mostly monounsaturated
487 fattyacids (C16:1, C18:1) and the low relative amount of polyunsaturated fatty acids
488 (C18:2, C18:3) could balance both these antagonistic requirements(Knothe, 2008). In
489 this view, the SCO produced by *L. starkeyi* in the present investigation, containing
490 about 55% of unsaturated fatty acids, appears a valid candidate for the production of
491 new generation biodiesel with good oxidative stability and cold flowproperties.
492 Moreover, in support of this perspective, the SCO resulted very similar to palm and
493 rapeseed oils (Anschau et al., 2014; Sutanto et al., 2018), usually employed as a
494 renewable source for the production of traditional biodiesel(Table 2).
495
496 *3.4 Mass balance of the processes*
497 Chemical and biological catalytic strategies implemented in this study allowed the
498 evaluation of anovelintegratedbiorefinery scheme for the valorisation of the
499 unpretreated lignocellulosic giant reed. The absence of the pretreatment step and the

optimisation of a cascade biomass exploitation would increase the economic sustainability and profitability of this biorefinery model. Moreover, the optimisation of tailored catalytic approaches for the production of second-generation sugars from both hemicellulose and cellulose fractionsand of new generation oil offered an important versatility in terms of technology and final high added-value biobased products.

For the first process step, namely the hemicellulose hydrolysis, the use of 27.6 g $FeCl_3 \cdot 6H_2O$, corresponding to 16.5 g $FeCl_3$, and 20 g Amberlyst-70 for 100 g of unpretreated giant reed (Figure 1), is justified by the absence of any chemical or hydrothermal pretreatment of the raw biomass. The adopted catalyst/biomass weight ratio of 0.17 and 0.20 wt/wt, for $FeCl_3$ and Amberlyst-70 respectively, are in agreement with those already reported in the literature for similar hydrolysis reactions. In particular, for the hemicellulose hydrolysis Kamireddy et al. (Kamireddy et al., 2013)adopted 20.3 g $FeCl_3$ for 105 g unpretreated corn stover, corresponding to the catalyst/biomass weight ratio of 0.19 wt/wt; Lòpez-Linares et al. (López-Linares et al., 2013)used 42.2 g $FeCl_3$ for 120 g unpretreated olive tree biomass, corresponding to the catalyst/biomass weight ratio of 0.35 wt/wt; Marcotullio et al. (Marcotullio et al., 2011)adopted 16.2 g $FeCl_3$ for 100 g unpretreated wheat straw, corresponding to the catalyst/biomass weight ratio of 0.16 wt/wt. Similar considerations can be performed for the hemicellulose hydrolysis catalysed by Amberlyst. You et al. (You et al., 2016)used 20 g Amberlyst35 DRY for 100 g of pretreated giant reed (110 °C, 1-n-butyl-3-methylimidazolium chloride, for 3 h), corresponding to the catalyst/biomass weight ratio of 0.20 wt/wt.In both cases, for $FeCl_3$ and Amberlyst-70, the employed catalyst/biomass weight ratios are comparable or even lower than literature reported values.Moreover, both catalysts can be recycled. In fact, an important advantage of

metal chlorides is represented by the possibility of being recovered as metal hydroxides by ultrafiltration. Metal hydroxides can be successively converted back to metal chlorides, when treated with conjugate acids (e.g. HCl), thus allowing the easy catalyst recycle and reuse in the process(Kamireddy et al., 2013). Regarding the heterogeneous catalyst adopted in the cascade process 2, previous research demonstrated that the embedded Amberlyst-70 can be separated by sieving and efficiently recycled by performing a simple washing with acetone, which represents a green and cheap solvent(Di Fidio et al., 2020c).

These aspects, together with the improvement of the SCO yield with respect to other processes involving the same yeast *L. starkeyi* DSM 70296, represent a promisingimprovement and innovation. Figure 1 shows the mass balance flow diagram of the twoadopted cascade processesbased on different catalytic strategies.Process 1, based on the combination of MW-assisted $FeCl_3$-catalysed hydrolysis of hemicellulose, enzymatic hydrolysis of the obtained cellulosic residue and yeast fermentation of X1 and G1, allowed the total production of 7.8 g of SCO from 100 gdry matter of raw biomass from giant reed cultivation, 4.7 g lipids deriving from the hemicellulose exploitation while 3.1 g from the cellulose valorisation. Process 2, based on the combination of MW-assisted Amberlyst-70-catalysed hydrolysis of hemicellulose, enzymatic hydrolysis of the obtained cellulosic residue and yeast fermentation of X2 and G2, allowed the total production of 7.7 g of SCO from the same amount and kind of biomass: 3.4 g lipids deriving from the hemicellulose exploitation, while 4.3 g from the cellulose valorisation. Thus, only considering the final SCO yield with respect to the starting unpretreated lignocellulosic biomass, the two proposed multi-step approaches resulted equivalent. The first one favoured the hemicellulose exploitation and was less

548 performing in the cellulose valorisation, while the second one favoured the cellulose
549 exploitation and was less efficient in the hemicellulose valorisation.A key aspect of this
550 multi-step approach consists in almost doubling the SCO production from the
551 lignocellulosic biomass due to the production of sugars from both hemicellulose and
552 cellulose and their biological conversion into lipids (Figure 1). This process strategy, up
553 to now never investigated, ensured a higher SCO production respect to those schemes
554 which performed a pretreatment step followed by the enzymatic hydrolysis of the
555 biomass and the hydrolysate fermentation (Azad et al., 2014; Pirozzi et al.,
556 2015).Regarding the SCO productivity, the values obtained in the present study, 2.6
557 g/day for both processes, were similar to those reported in the literature for the same
558 yeast species. In particular, the work of Sutanto et al. (Sutanto et al., 2018)on *L. starkeyi*
559 reported the productivity values in the range 0.04-4.00 g/day. Moreover, the same
560 review reported for the yeast strain DSM 70296 values in the range 0.65-1.44
561 g/day.Figure 4 shows the kinetics of the lipids production rate as a function of type of
562 hydrolysate (X1, X2, G1 and G2) and the statistical analysis of the results through
563 thetwo-way ANOVA.
564 (Figure 4, near here)
565 No statistically significant difference was observed at 24 h among the four hydrolysates.
566 On the contrary, the lipids production rate observed at 48 h for G1 (around 3.5 g/L/day)
567 and G2 (around 4.5 g/L/day) was significantly higher than those reached for X1 and X2
568 (around 1.0 g/L/day). At the same time, the values achieved from G1 and G2 were not
569 statistically different from each other, as well as those obtained from X1 and X2. At 72
570 h, the lipids production rate for X2 was significantly higher than the values obtained for
571 the other hydrolysates. Moreover, the production rates of X1 (around 2.5 g/L/day) and

G2 (around 2.0 g/L/day) were not statistically different from each other. The production rate from G1 (around 0.5 g/L/day) was the lowest one after 3 days. Considering the kinetics within the same hydrolysate, for the two xylose-rich hydrolysates the maximum lipids production rate was reached at 72 h with an increase that resulted statistically different than the values achieved at 24 and 48 h. Differently, for the two glucose-rich hydrolysates, the maximum lipids production rate was reached at 48 h, which resulted significantly different from the values obtained after 24 and 72 h. Finally, in the case of X2, the difference in the production rate between 72 and 96 h was not statistically different.

On this basis, this integrated cascade process can offer an outstanding opportunity for the exploitation of all the biomasses characterised by a relevant amount of hemicellulose,of which giant reed is a representative example,thus allowing case-specificselection of suitable feedstocks among a variety of similar lignocellulosic crops and residuesfor this type of biorefinery processes.Considering that giant reed under suited pedoclimatic conditions is able to produce 37.7 tonsdry matter ha^{-1} yr^{-1}, as 12-year average under low input and rainfed conditions(Nassi o Di Nasso et al., 2011), the potential SCO production could equal 2.9 tons $ha^{-1}yr^{-1}$. Under similar conditions, an annual oleaginous crop, such as sunflower, can deliver no more than 2 tons ha^{-1} yr^{-1} of high oleic oil. These results indicate that such process, based onunconventional renewable biomass resources, mild reaction conditions, water as the solvent, safe catalysts, microwaves as an efficient energy system, has the potential to achieve yields similar to conventional oil crops respecting the principles of Green Chemistry.

The integral use of biomass is essential to ensure sustainability in such supply chains.At this regard, both the adopted approaches can lead to the production of lignin-rich solid

residues after the cellulose hydrolysis,which can further be exploited to give valuable aromatic compounds. Analogously, both approaches may lead to the production of a huge amount of spent cell biomass after the oil extraction, similar to the yeast extract produced from spent brewer's yeast(Tanguler & Erten, 2008) and spent baker's yeast(Vukašinović-Milić et al., 2007). This spent biomasscould suit for nitrogen recovery in the fermentation process or forbiomethane production by anaerobic digestion(Moeller et al., 2018; Sosa-Hernández et al., 2016). Moreover, process 2 could also provide furfural, which represents one of the most promising platform chemicals directlyderived from biomass(Wang et al., 2019).

4. Conclusions

This study reported for the first time two alternative multi-step conversions of unpretreated giant reed to SCO. The conversion of hemicellulose and cellulose fractions into xylose- and glucose-rich hydrolysates with the low production of by-products enabled the fermentation of producedundetoxified hydrolysates by *L. starkeyi*. Sugars exhaustion was reached for all the hydrolysates, providing good lipid yields,15-24 wt%, and oil content,about30 wt%. The two cascade processes enabled us to achieveabout 8 g SCO from 100 g raw biomass. This SCO represents an outstanding alternative to fossil and food oils for the production of biofuels and bioproducts.

Acknowledgements

The authors acknowledgeProf. Pierdomenico Perata and Dr.Silvia Gonzali of the Institute of Life Sciences (Sant'Anna School ofAdvanced Study)for the kind hospitality andsupport in the PlantLab laboratories.

Appendix A. Supplementary data

E-supplementary data of this work can be found in the online version of the paper.

References

1. Angerbauer, C., Siebenhofer, M., Mittelbach, M., Guebitz, G., 2008. Conversion of sewage sludge into lipids by *Lipomyces starkeyi* for biodiesel production. Bioresour. Technol. 99, 3051-3056.
2. Anschau, A., Xavier, M.C., Hernalsteens, S., Franco, T.T., 2014. Effect of feeding strategies on lipid production by *Lipomyces starkeyi*. Bioresour. Technol. 157, 214-222.
3. Azad, A., Yousuf, A., Ferdoush, A., Hasan, M., Karim, M., Jahan, A., 2014. Production of microbial lipids from rice straw hydrolysates by *Lipomyces starkeyi* for biodiesel synthesis. J. Microb. Biochem. Technol. 8, 1-6.
4. Bonturi, N., Matsakas, L., Nilsson, R., Christakopoulos, P., Miranda, E.A., Berglund, K.A., Rova, U., 2015. Single cell oil producing yeasts *Lipomyces starkeyi* and *Rhodosporidium toruloides*: selection of extraction strategies and biodiesel property prediction. Energies 8, 5040-5052.
5. Bosco, S., Nassi o Di Nasso, N., Roncucci, N., Mazzoncini, M., Bonari, E., 2016. Environmental performances of giant reed (*Arundo donax* L.) cultivated in fertile and marginal lands: A case study in the Mediterranean. Eur. J. Agron. 78, 20-31.
6. Calvey, C.H., Su, Y.K., Willis, L.B., McGee, M., Jeffries, T.W., 2016. Nitrogen limitation, oxygen limitation, and lipid accumulation in *Lipomyces starkeyi*. Bioresour. Technol. 200, 780-788.

644 7. Ceotto, E., Marchetti, R., Castelli, F., 2018. Residual soil nitrate as affected by giant
645 reed cultivation and cattle slurry fertilization. Ital. J. Agron. 13, 1264-1270.
646 8. d'Espaux, L., Mendez-Perez, D., Li, R., Keasling, J.D., 2015. Synthetic biology for
647 microbial production of lipid-based biofuels. Curr. Opin. Chem. Biol. 29, 58-65.
648 9. Di Fidio, N., Antonetti, C., Raspolli Galletti, A.M., 2019. Microwave-assisted
649 cascade exploitation of giant reed (*Arundo donax* L.) to xylose and levulinic acid
650 catalysed by ferric chloride. Bioresour. Technol. 293, 122050-122058.
651 10. Di Fidio, N., Dragoni, F., Antonetti, C., De Bari, I., Raspolli Galletti, A.M.,
652 Ragaglini, G., 2020a. From paper mill waste to single cell oil: enzymatic hydrolysis
653 to sugars and their fermentation into microbial oil by the yeast *Lipomyces starkeyi*.
654 Bioresour. Technol. 315, 123790-123798.
655 11. Di Fidio, N., Fulignati, S., De Bari, I., Antonetti, C., Raspolli Galletti, A.M., 2020b.
656 Optimisation of glucose and levulinic acid production from the cellulose fraction of
657 giant reed (*Arundo donax* L.) performed in the presence of ferric chloride under
658 microwave heating. Bioresour. Technol. 313, 123650-123658.
659 12. Di Fidio, N., Raspolli Galletti, A.M., Fulignati, S., Licursi, D., Liuzzi, F., De Bari,
660 I., Antonetti, C., 2020c. Multi-Step Exploitation of Raw *Arundo donax* L. for the
661 Selective Synthesis of Second-Generation Sugars by Chemical and Biological
662 Route. Catalysts 10, 79-102.
663 13. Gong, Z., Wang, Q., Shen, H., Hu, C., Jin, G., Zhao, Z.K., 2012. Co-fermentation of
664 cellobiose and xylose by *Lipomyces starkeyi* for lipid production. Bioresour.
665 Technol. 117, 20-24.
666 14. Gong, Z., Wang, Q., Shen, H., Wang, L., Xie, H., Zhao, Z.K., 2014. Conversion of
667 biomass-derived oligosaccharides into lipids. Biotechnol. Biofuels 7, 13-22.

15. Javaid, H., Manzoor, M., Qazi, J., Xiaochao, X., Tabssum, F., 2017. Potential of oleaginous yeasts as economic feedstock for biodiesel production. Biologia 63, 217-234.
16. Kamireddy, S.R., Li, J., Tucker, M., Degenstein, J., Ji, Y., 2013. Effects and mechanism of metal chloride salts on pretreatment and enzymatic digestibility of corn stover. Ind. Eng. Chem. Res. 52, 1775-1782.
17. Knothe, G., 2008. "Designer" biodiesel: optimizing fatty ester composition to improve fuel properties. Energy Fuels 22, 1358-1364.
18. Leiva-Candia, D., Tsakona, S., Kopsahelis, N., Garcia, I., Papanikolaou, S., Dorado, M., Koutinas, A., 2015. Biorefining of by-product streams from sunflower-based biodiesel production plants for integrated synthesis of microbial oil and value-added co-products. Bioresour. Technol. 190, 57-65.
19. Loow, Y.L., Wu, T.Y., Tan, K.A., Lim, Y.S., Siow, L.F., Md. Jahim, J., Mohammad, A.W., Teoh, W.H., 2015. Recent advances in the application of inorganic salt pretreatment for transforming lignocellulosic biomass into reducing sugars. J. Agric. Food Chem. 63, 8349-8363.
20. López-Linares, J.C., Romero, I., Moya, M., Cara, C., Ruiz, E., Castro, E., 2013. Pretreatment of olive tree biomass with $FeCl_3$ prior enzymatic hydrolysis. Bioresour.Technol. 128, 180-187.
21. Mahlia, T., Syazmi, Z., Mofijur, M., Abas, A.P., Bilad, M., Ong, H.C., Silitonga, A., 2020. Patent landscape review on biodiesel production: Technology updates. Renew. Sust. Energ. Rev. 118, 109526-109534.
22. Marcotullio, G., Krisanti, E., Giuntoli, J., De Jong, W., 2011. Selective production of hemicellulose-derived carbohydrates from wheat straw using dilute HCl or $FeCl_3$

692 solutions under mild conditions. X-ray and thermo-gravimetric analysis of the solid
693 residues. Bioresour.Technol. 102, 5917-5923.
694 23. Meena, S., Navatha, S., Devi, B.P., Prasad, R., Pandey, A., Sukumaran, R., 2015.
695 Evaluation of Amberlyst15 for hydrolysis of alkali pretreated rice straw and
696 fermentation to ethanol. Biochem. Eng. J. 102, 49-53.
697 24. Moeller, L., Bauer, A., Zehnsdorf, A., Lee, M.Y., Müller, R.A., 2018. Anaerobic
698 co-digestion of waste yeast biomass from citric acid production and waste frying fat.
699 Eng. Life Sci. 18, 425-433.
700 25. Nassi o Di Nasso, N., Roncucci, N., Triana, F., Tozzini, C., Bonari, E., 2011.
701 Seasonal nutrient dynamics and biomass quality of giant reed (*Arundo donax* L.)
702 and miscanthus (*Miscanthus* × *giganteus* Greef et Deuter) as energy crops. Ital. J.
703 Agron. 6, 24-30.
704 26. Papanikolaou, S., Aggelis, G., 2011. Lipids of oleaginous yeasts. Part I:
705 Biochemistry of single cell oil production. Eur. J. Lipid Sci. Technol. 113, 1031-
706 1051.
707 27. Patel, A., Karageorgou, D., Rova, E., Katapodis, P., Rova, U., Christakopoulos, P.,
708 Matsakas, L., 2020. An Overview of Potential Oleaginous Microorganisms and
709 Their Role in Biodiesel and Omega-3 Fatty Acid-Based Industries. Microorganisms
710 8, 434-473.
711 28. Pilu, R., Cassani, E., Landoni, M., Badone, F.C., Passera, A., Cantaluppi, E., Corno,
712 L., Adani, F., 2014. Genetic characterization of an Italian Giant Reed (*Arundo*
713 *donax* L.) clones collection: exploiting clonal selection. Euphytica 196, 169-181.

714 29. Pirozzi, D., Ausiello, A., Yousuf, A., Zuccaro, G., Toscano, G., 2014a. Exploitation
715 of oleaginous yeasts for the production of microbial oils from agricultural biomass.
716 Chem. Eng. 37, 469-474.
717 30. Pirozzi, D., Fiorentino, N., Impagliazzo, A., Sannino, F., Yousuf, A., Zuccaro, G.,
718 Fagnano, M., 2015. Lipid production from *Arundo donax* grown under different
719 agronomical conditions. Renew. Energy 77, 456-462.
720 31. Pirozzi, D., Sagnelli, D., Sannino, F., Toscano, G., 2014b. Study of a Discontinuous
721 Fed-Batch Fermentor for the Exploitation of Agricultural Biomasses to Produce II-
722 Generation. Chem. Eng. 38, 169-174.
723 32. Probst, K.V., Schulte, L.R., Durrett, T.P., Rezac, M.E., Vadlani, P.V., 2016.
724 Oleaginous yeast: a value-added platform for renewable oils. Crit. Rev. Biotechnol.
725 36, 942-955.
726 33. Qi, X., Yan, L., Shen, F., Qiu, M., 2019. Mechanochemical-assisted hydrolysis of
727 pretreated rice straw into glucose and xylose in water by weakly acidic solid
728 catalyst. Bioresour.Technol. 273, 687-691.
729 34. Scordia, D., Cosentino, S.L., 2019. Perennial energy grasses: resilient crops in a
730 changing European agriculture. Agriculture 9, 169-187.
731 35. Serrano, M., Oliveros, R., Sánchez, M., Moraschini, A., Martínez, M., Aracil, J.,
732 2014. Influence of blending vegetable oil methyl esters on biodiesel fuel properties:
733 oxidative stability and cold flow properties. Energy 65, 109-115.
734 36. Sosa-Hernández, O., Parameswaran, P., Alemán-Nava, G.S., Torres, C.I., Parra-
735 Saldívar, R., 2016. Evaluating biochemical methane production from brewer's spent
736 yeast. J. Ind. Microbiol. Biotechnol. 43, 1195-1204.

37. Sutanto, S., Zullaikah, S., Tran-Nguyen, P.L., Ismadji, S., Ju, Y.H., 2018. *Lipomyces starkeyi*: its current status as a potential oil producer. Fuel Process. Technol. 177, 39-55.

38. Takaku, H., Matsuzawa, T., Yaoi, K., Yamazaki, H., 2020. Lipid metabolism of the oleaginous yeast *Lipomyces starkeyi*. Appl. Microbiol. Biotechnol. 104, 6141-6148.

39. Tanguler, H., Erten, H., 2008. Utilisation of spent brewer's yeast for yeast extract production by autolysis: The effect of temperature. Food Bioprod.Process. 86, 317-321.

40. Tapia, E., Anschau, A., Coradini, A.L., Franco, T.T., Deckmann, A.C., 2012. Optimization of lipid production by the oleaginous yeast *Lipomyces starkeyi* by random mutagenesis coupled to cerulenin screening. AMB Express 2, 64-71.

41. Vieira, J., Ienczak, J., Rossell, C., Pradella, J., Franco, T., 2014. Microbial lipid production: screening with yeasts grown on Brazilian molasses. Biotechnol. Lett. 36, 2433-2442.

42. Vukašinović-Milić, T., Rakin, M., Šiler-Marinković, S., 2007. Utilization of baker's yeast (*Saccharomyces cerevisiae*) for the production of yeast extract: effects of different enzymatic treatments on solid, protein and carbohydrate recovery. J. Serb. Chem. Soc. 72, 451-457.

43. Wang, R., Wang, J., Xu, R., Fang, Z., Liu, A., 2014. Oil production by the oleaginous yeast *Lipomyces starkeyi* using diverse carbon sources. Bioresources 9, 7027-7040.

44. Wang, Y., Zhao, D., Rodríguez-Padrón, D., Len, C., 2019. Recent advances in catalytic hydrogenation of furfural. Catalysts 9, 796-828.

45. Wild, R., Patil, S., Popović, M., Zappi, M., Dufreche, S., Bajpai, R., 2010. Lipids from *Lipomyces starkeyi*. Food Technol. Biotechnol. 48, 329-335.
46. Xavier, M., Coradini, A., Deckmann, A., Franco, T., 2017. Lipid production from hemicellulose hydrolysate and acetic acid by *Lipomyces starkeyi* and the ability of yeast to metabolize inhibitors. Biochem. Eng. J. 118, 11-19.
47. Xavier, M.C., Franco, T.T., 2014. Batch and continuous culture of hemicellulosic hydrolysate from sugarcane bagasse for lipids production. Chem. Eng. Trans. 38, 385-390.
48. Yang, B., Tao, L., Wyman, C.E., 2018. Strengths, challenges, and opportunities for hydrothermal pretreatment in lignocellulosic biorefineries. Biofuel. Bioprod. Biorefin. 12, 125-138.
49. You, T., Shao, L., Wang, R., Zhang, L., Xu, F., 2016. Facile isothermal solid acid catalyzed ionic liquid pretreatments to enhance the combined sugars production from *Arundo donax* Linn. Biotechnol. Biofuels 9, 177-189.
50. Zhao, X., Kong, X., Hua, Y., Feng, B., Zhao, Z., 2008. Medium optimization for lipid production through co-fermentation of glucose and xylose by the oleaginous yeast *Lipomyces starkeyi*. Eur. J. Lipid Sci. Technol. 110, 405-412.

Captions for Figures

Fig.1. Flow diagram and mass balance of the different chemical and biological catalytic steps adopted for the production of single cell oil from giant reed.

Fig. 2. Glucose, xylose, dry cell weight (DCW) and lipids concentrations (g/L), and lipid content (wt%) during the fermentation of X1 (A), X2 (B), G1 (C) and G2 (D)by *L. starkeyi*DSM 70296.

Fig. 3. Dry cell weight concentration (g/L), lipids concentration (g/L), lipid contents (wt%) and maximum lipids production (g/L/day) at the end of the fermentation of X1, X2, G1 and G2 hydrolysates. Different letters on the bars indicate significant differences (* $p < 0.05$; ** $p < 0.01$; *** $p < 0.001$).

Fig. 4. Kinetics of the maximum lipids production (g/L/day) as a function of the type of the fermented hydrolysate (X1, X2, G1 and G2). Different letters on the values indicate significant differences (* $p < 0.05$) in the same kinetics (lowercase letters) or at the same process time (uppercase letters).

Table 1

Chemical composition of giant reed hydrolysates obtained by different catalytic approaches and used as fermentation substrates.

Giant reed hydrolysate	Glucose (g/L)	Xylose (g/L)	Furfural (g/L)	5-HMF (g/L)	Acetic acid (g/L)	Formic acid (g/L)	Levulinic acid (g/L)
X1[a]	5.6±0.2	19.4±0.3	0.3±0.0	0.4±0.0	2.2±0.2	0.5±0.0	n.d.
X2[b]	8.0±0.3	38.0±0.5	1.0±0.1	1.3±0.1	4.7±0.4	1.0±0.1	0.5±0.0
X2[b*]	8.0±0.2	38.0±0.4	n.d.	1.3±0.2	n.d.	1.0±0.2	0.5±0.0
G1c	21.8±0.4	n.d.	n.d.	n.d.	n.d.	n.d.	n.d.
G2[d]	32.8±0.7	n.d.	n.d.	n.d.	n.d.	n.d.	n.d.

[a]Hydrolysate obtained by microwave-assisted $FeCl_3$-catalysed hemicellulose hydrolysis; [b]hydrolysate obtained by microwave-assisted Amberlyst-70-catalysed hemicellulose hydrolysis; [c]hydrolysate obtained by enzymatic hydrolysis of the cellulose-rich residue after the microwave-assisted $FeCl_3$-catalysed hemicellulose hydrolysis; [d]hydrolysate obtained by enzymatic hydrolysis of the cellulose-rich residue after the microwave-assisted Amberlyst-70-catalysed hemicellulose hydrolysis; n.d. = not detected.

*X2 after the selective removal of furfural and acetic acid by vacuum evaporation.

807 **Table 2**

808 Chemical composition (wt%) of single cell oils obtained by fermentation of different
809 xylose- and glucose-rich hydrolysates and their comparison with traditional food oils
810 used for the biodiesel production.

Oil	C16:0	C16:1	C18:0	C18:1	C18:2
SCO from X1	37.6	3.5	7.2	47.5	4.2
SCO from X2	34.6	3.1	7.6	49.5	5.2
SCO from G1	35.8	2.5	8.1	50.5	3.1
SCO from G2	31.8	8.0	5.1	48.3	6.8
Palm oil[a]	36.7	0.1	6.6	46.1	8.6
Rapeseed oil[a]	40.1	0.1	4.1	43.0	11.0

811 [a]FAMEs profiles referred to the work of Sutanto et al. (Sutanto et al., 2018).

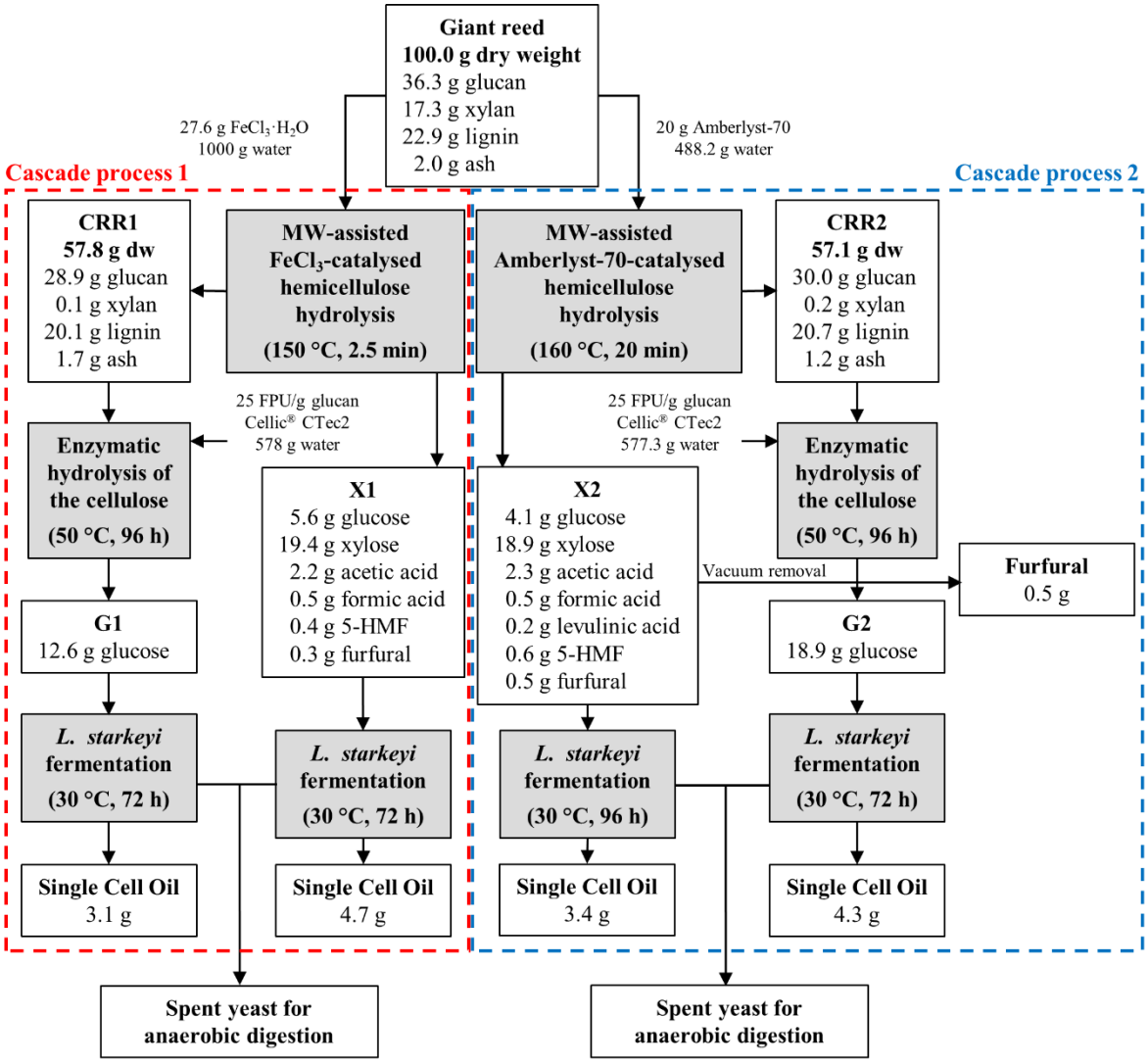
Giant reed
100.0 g dry weight
36.3 g glucan
17.3 g xylan
22.9 g lignin
2.0 g ash
27.6 g FeCl3·H2O
1000 g water
20 g Amberlyst-70
488.2 g water
Cascade process 1
Cascade process 2
CRR1
57.8 g dw
28.9 g glucan
0.1 g xylan
20.1 g lignin
1.7 g ash
MW-assisted FeCl3-catalysed hemicellulose hydrolysis
(150 °C, 2.5 min)
MW-assisted Amberlyst-70-catalysed hemicellulose hydrolysis
(160 °C, 20 min)
CRR2
57.1 g dw
30.0 g glucan
0.2 g xylan
20.7 g lignin
1.2 g ash
25 FPU/g glucan
Cellic® CTec2
578 g water
25 FPU/g glucan
Cellic® CTec2
577.3 g water
Enzymatic hydrolysis of the cellulose
(50 °C, 96 h)
Enzymatic hydrolysis of the cellulose
(50 °C, 96 h)
X1
5.6 g glucose
19.4 g xylose
2.2 g acetic acid
0.5 g formic acid
0.4 g 5-HMF
0.3 g furfural
X2
4.1 g glucose
18.9 g xylose
2.3 g acetic acid
0.5 g formic acid
0.2 g levulinic acid
0.6 g 5-HMF
0.5 g furfural
Vacuum removal
Furfural
0.5 g
G1
12.6 g glucose
G2
18.9 g glucose
L. starkeyi fermentation
(30 °C, 72 h)
L. starkeyi fermentation
(30 °C, 72 h)
L. starkeyi fermentation
(30 °C, 96 h)
L. starkeyi fermentation
(30 °C, 72 h)
Single Cell Oil
3.1 g
Single Cell Oil
4.7 g
Single Cell Oil
3.4 g
Single Cell Oil
4.3 g
Spent yeast for anaerobic digestion
Spent yeast for anaerobic digestion

Figure 1

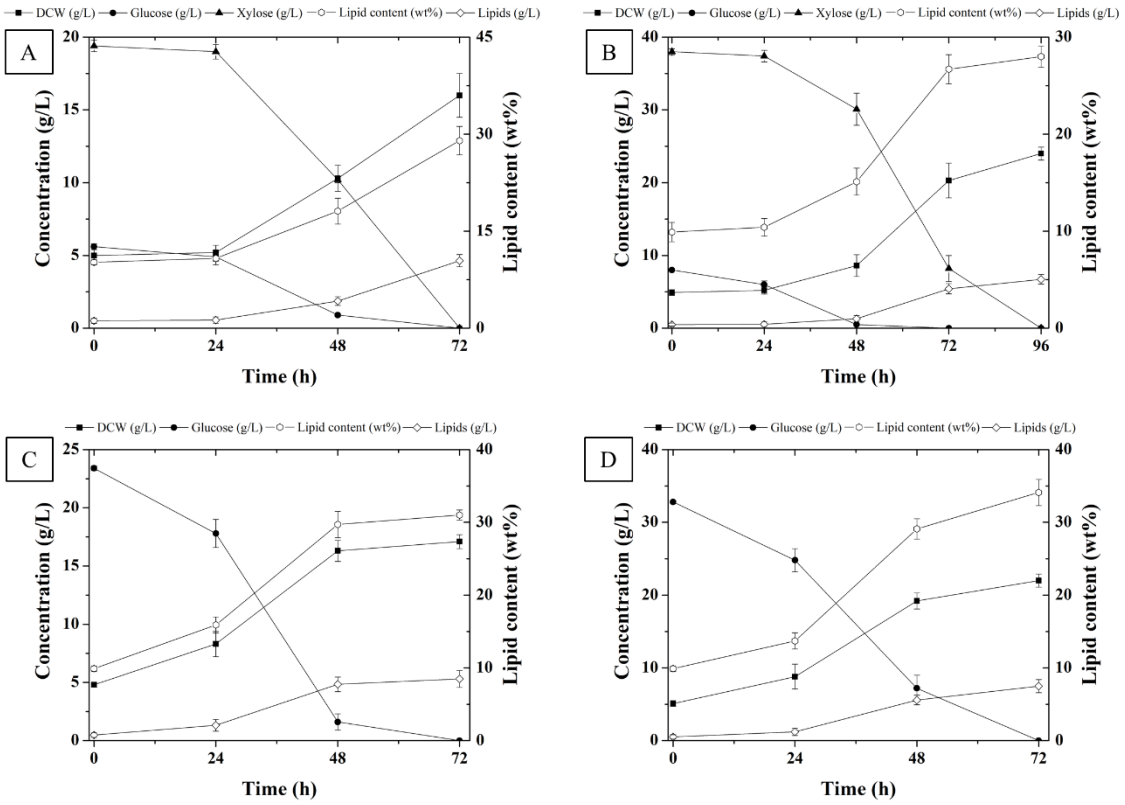
DCW (g/L)
Glucose (g/L)
Xylose (g/L)
Lipid content (wt%)
Lipids (g/L)
A
B
C
D
Concentration (g/L)
Lipid content (wt%)
Time (h)

Figure 2

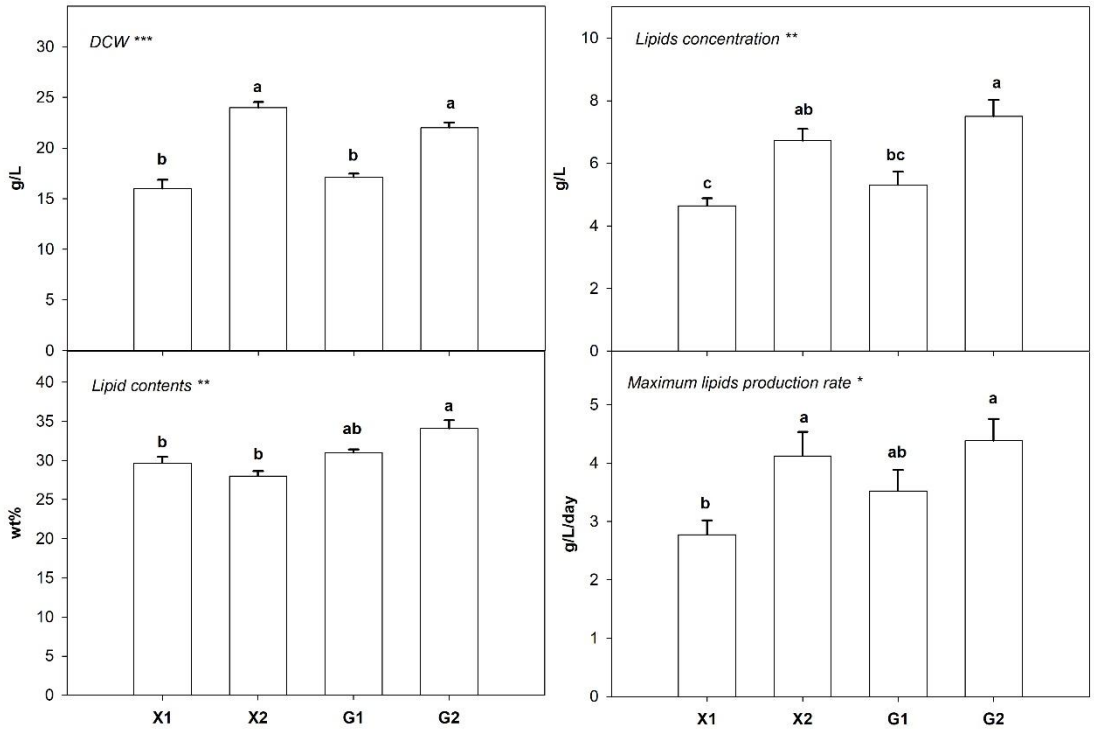
DCW ***
g/L
b
a
b
a
Lipids concentration **
g/L
c
ab
bc
a
Lipid contents **
wt%
b
b
ab
a
Maximum lipids production rate *
g/L/day
b
a
ab
a
X1
X2
G1
G2

Figure 3

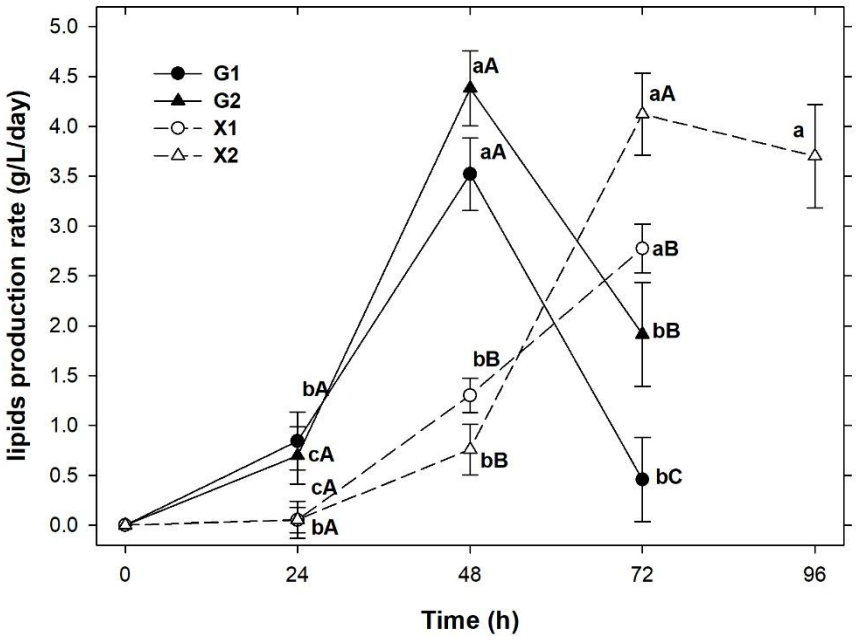

849
850 **Figure 4**

851

852